Experimental Performance Evaluation of Geotechnical Encased Columns

Etienne Gonzalez[1]; Abdurrahman Almikati, Ph.D.[2];
and Jorge Gabriel Zornberg, P.E., F.ASCE[3]

[1]Ph.D. Candidate, Dept. of Civil, Architectural, and Environmental Engineering, Univ. of Texas at Austin. Email: etienne.gonzalez@utexas.edu
[2]Lecturer, Ingram School of Engineering, Texas State Univ. Email: abedmikati@txstate.edu
[3]Priddy Centennial Professor, Dept. of Civil, Architectural, and Environmental Engineering, Univ. of Texas at Austin. Email: zornberg@mail.utexas.edu

ABSTRACT

This study investigated the performance of geosynthetic encased columns (GECs) in soft soils using physical models with a transparent clay surrogate. The objective was to identify optimal design conditions that maximize the stabilization provided by the encasement while minimizing risks associated with insufficient or excessive reinforcement. Two representative GEC models were selected to illustrate different performance outcomes: a baseline model with medium stiffness encasement and a model with high stiffness encasement. Detailed examination of these models highlighted the importance of tailoring encasement confinement to facilitate performance gains while avoiding over-design. Encasement tensile strength significantly reduced column bulging compared to unreinforced and low-stiffness models. Mobilized encasement confinement enabled constant incremental bearing capacity enhancements, provided tensile strains remained within allowable limits. High-stiffness encasement models achieved rapid confinement mobilization at lower strains due to the steep tensile strength-strain slope. Column infill deviatoric stress versus axial strain relationships captured performance and onset of column failure in detail. Results demonstrated encasement tensile capacity controls GEC failure in very soft soils, with bearing capacity depending primarily on encasement stiffness and strength rather than column infill properties.

INTRODUCTION

Geosynthetic encased columns (GECs) are an innovative ground improvement technique that has gained increasing popularity for supporting embankments and structures on soft soils. GECs consist of granular columns confined by a geosynthetic encasement, which provides additional lateral support to the column material. The encasement enhances the load-bearing capacity and stiffness of the columns while minimizing lateral deformations, leading to improved overall performance compared to conventional stone columns (Raithel & Kempfert, 2000; Murugesan & Rajagopal, 2006; Yoo & Kim, 2009).

Previous studies have demonstrated the effectiveness of GECs in reducing settlements and improving bearing capacity through field measurements, laboratory tests, and numerical simulations (Alexiew et al., 2005; Gniel & Bouazza, 2009; Araujo et al., 2009; Khabbazian et al., 2010; Pulko et al., 2011; Almeida et al., 2015). These studies have primarily focused on the global performance of GEC-reinforced soil systems, providing valuable insights into the load transfer mechanisms and the influence of key design parameters such as encasement stiffness, column diameter, and area replacement ratio.

However, there is still a need for a more detailed understanding of the local interactions between the GEC components (encasement, column infill, and surrounding soil) and the development of failure mechanisms under various loading conditions. Physical modeling using transparent soil surrogates offers a promising approach to investigate these aspects, as it allows for direct visual observation and quantitative measurement of deformations and strains within the GEC system (Iskander, 2010; Gill et al., 2014; Stanier & White, 2013).

This study aims to evaluate the performance of GECs in soft soils using a larger-scale physical model with a transparent clay surrogate. The main objectives are to:

1. Investigate the local deformation and strain patterns within GECs under undrained loading conditions
2. Identify optimal design conditions that maximize the stabilizing effect of the encasement while minimizing potential risks associated with insufficient or excessive reinforcement
3. Examine the influence of encasement stiffness on the failure mechanisms and overall performance of GECs

Two representative GEC models, featuring medium and high stiffness encasements, are selected for detailed analysis. Digital image correlation (DIC) techniques are employed to obtain visual and quantitative insights into the column behavior, failure mechanisms, and the effect of design parameters on GEC performance. The results provide valuable guidance for optimizing the design of GEC systems in soft soil conditions.

MATERIALS USED

The experimental setup consists of a custom-designed transparent unit cell chamber mounted on a modified triaxial testing system. The unit cell has an inner diameter of 200 mm and a height of 500 mm. The chamber is filled with a transparent clay surrogate, which is a mixture of laponite powder, distilled water and Sodium Pyrophosphate (SPP). The laponite mixture is prepared at a concentration of 10% by weight, resulting in an undrained shear strength of approximately 1.5 kPa, simulating the behavior of a very soft clay deposit.

The column material used in the GEC models is a uniformly graded Monterey sand with a mean particle size of 0.6 mm. The sand is installed at a relative density of 85%. The geosynthetic encasements are made of a polyester geotextile with secant stiffness values ($J_{5\%}$) ranging from 8 to 70 kN/m. Four different encasement types are considered in the study: GTX08, GTX11, GTX34, and GTX70, corresponding to secant stiffness values of 8, 11, 34, and 70 kN/m, respectively.

The GEC models are installed in the unit cell chamber shown in Figure 1a &1b, using a specially designed formwork that ensures a uniform column diameter and a vertical alignment. The formwork is gradually lifted as the sand is poured in layers and compacted to the desired density. The encasement is wrapped around the column with a 20 mm overlap, using a polyester glue.

TESTING PROGRAM

The testing program focuses on evaluating the performance of two representative GEC models:

1. B-GEC-J34: Baseline model with a medium stiffness GTX34 encasement ($J_{5\%}$ = 34 kN/m)
2. B-GEC-J70: Model with a high stiffness GTX70 encasement ($J_{5\%}$ = 70 kN/m)

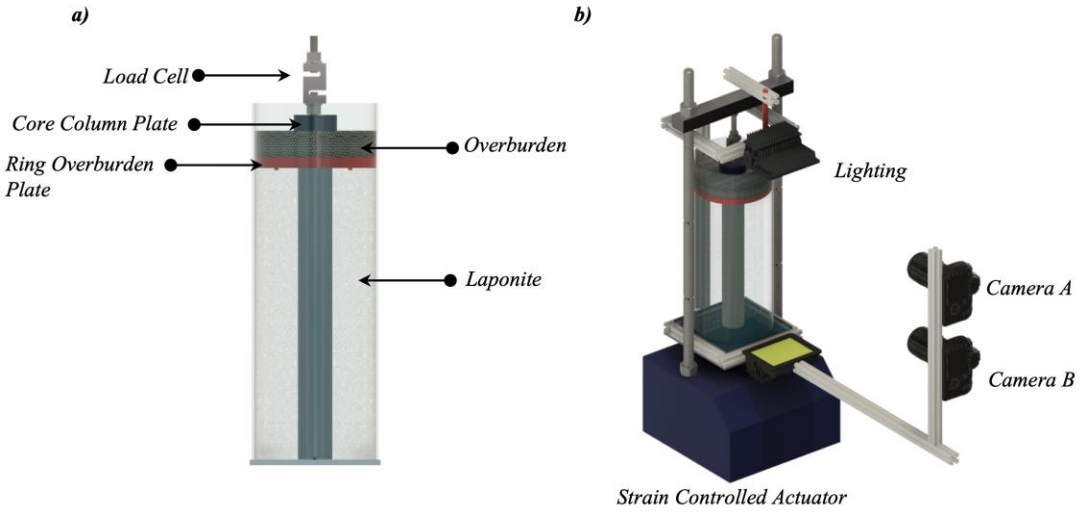

Figure 1: Schematic Drawings of the Setup Showing (a) Unit Cell Chamber and (b) Configuration of the Testing Setup

Both models have a column diameter of 80 mm and a length of 500 mm, resulting in an aspect ratio (L/D) of 6.25. The columns are installed in the laponite clay surrogate and subjected to undrained vertical loading applied through a rigid plate at the top of the column. The loading is applied in displacement control at a rate of 1 mm/min.

During the tests, the load-displacement response of the GEC models is continuously monitored using a load cell and a LVDT. Digital images of the GEC models are captured at regular intervals using high-resolution cameras positioned around the transparent unit cell chamber. The images are processed using DIC techniques to obtain full-field displacement and strain measurements within the GEC system.

RESULTS AND ANALYSIS

GEC Baseline Model (B-GEC-J34)

The baseline model with a medium stiffness GTX34 encasement exhibited a remarkable performance, showing no signs of failure up to an axial strain of 10% under high vertical loads. The load-displacement response (Figure 2a) indicated a steady increase in the top column vertical pressure applied with increasing column axial strain, without any significant plateaus or drops that would suggest a loss of stability. The encasement radial strain profiles (Figure 3a) revealed a nearly uniform distribution of strains along the column length up to an axial strain of 8%. Only minor bulging was observed in the upper part of the column, with no visible damage to the encasement. This suggests that the encasement effectively contained the lateral deformation of the column material, preventing the development of localized failure zones.

Comparing the performance of the B-GEC-J34 model with unreinforced and low stiffness encasement models (not shown here) highlights the significant role of encasement tensile strength in reducing column bulging. The medium stiffness encasement provided sufficient lateral support to the column material, allowing for a more uniform distribution of stresses and strains within the GEC system. It is important to note that the presence of bulging does not

necessarily indicate an overall failure of the GEC. Failure occurs only when the encasement yields or breaks, leading to a loss of confinement and a rapid increase in lateral deformations. In the case of the B-GEC-J34 model, the mobilized encasement confining stresses were able to prevent outright failure by limiting the lateral deformation to permissible levels.

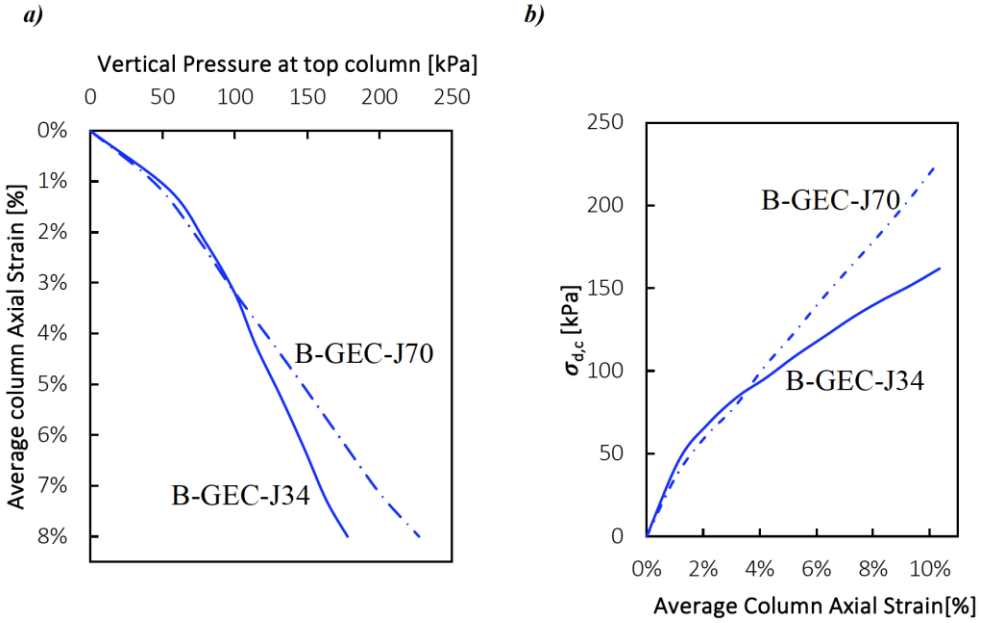

Figure 2: Bearing behavior of models: B-GEC-J34 and B-GEC-J70, a) Load-Settlement response, b) Column infill deviatoric Stress-Average column axial strain

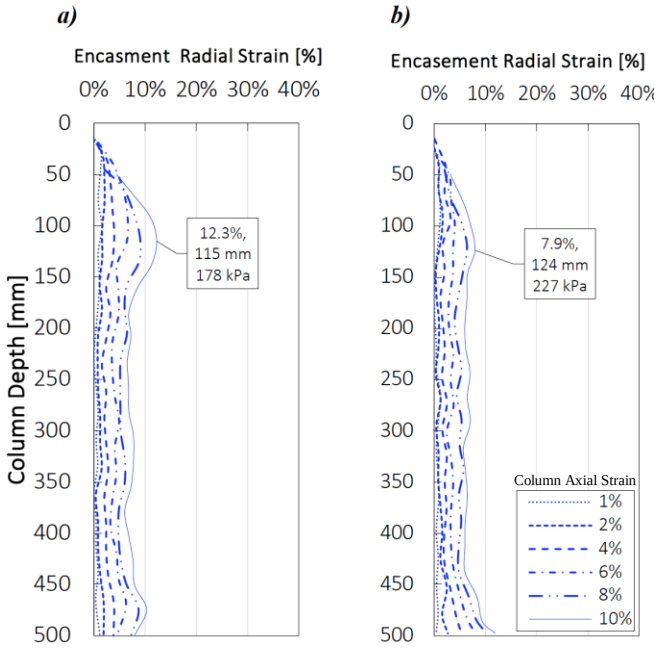

Figure 3: Profiles of geosynthetic encasement radial strain of models: a) B-GEC-J34, and b) B-GEC-J70

The results suggest that the GTX34 encasement effectively delivered stabilization to the GEC system without suffering damage, even under significant axial deformations. The encasement mobilized approximately 90% of its available tensile strength, indicating an optimal utilization of the reinforcement capacity.

GEC with High Stiffness Encasement (B-GEC-J70)

The GEC model with a high stiffness GTX70 encasement (B-GEC-J70) demonstrated an even better performance compared to the baseline model. No signs of tensile breakage or damage were observed in the encasement up to an axial strain of 10%, indicating a highly stable and resilient GEC system. The load-displacement response (Figure 2b) of the B-GEC-J70 model showed a similar trend to the baseline model up to a column axial strain of 3.5%. However, beyond this point, the high stiffness encasement model exhibited a steeper increase in the top column vertical pressure applied, suggesting a more rapid mobilization of the encasement confinement. The encasement radial strain profiles (Figure 3b) revealed a uniform distribution of strains along the entire column length, with no evidence of localized bulging or shear plane development. The maximum radial strains measured in the B-GEC-J70 model were consistently lower than those observed in the baseline model, indicating a more effective containment of the lateral deformation. The superior performance of the B-GEC-J70 model can be attributed to the high stiffness of the GTX70 encasement, which resulted in a rapid mobilization of confinement at lower axial strains. The steep tensile strength-strain slope of the GTX70 encasement allowed for a more efficient transfer of loads from the column material to the encasement, leading to a uniform distribution of stresses and strains within the GEC.

The results suggest that the GTX70 encasement remained in the elastic range throughout the loading process, mobilizing only a fraction of its ultimate tensile strength. This indicates a potential for further optimization of the encasement design, as the high stiffness encasement may be over-designed for the given loading conditions.

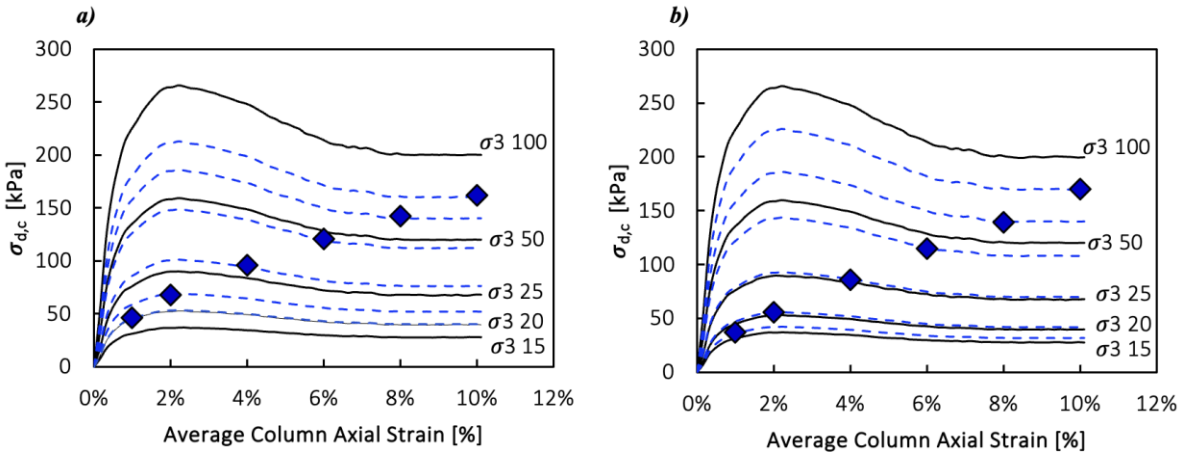

Figure 4: Column infill mobilization from models: a) B-GEC-J34 baseline & b)B-GEC-J70

Column Infill Stress State

To gain further insights into the stress-strain behavior of the GEC models, the column infill deviatoric stress versus axial strain relationships were analyzed (Figure 4). This approach

provides a more detailed representation of the true stress state within the column material, considering both the vertical stress and the mobilized lateral confinement.

The deviatoric stress-strain curves for both the B-GEC-J34 and B-GEC-J70 models exhibited a similar trend, with an initial linear elastic response followed by a gradual yielding and a plateau at larger strains. The B-GEC-J70 model achieved higher deviatoric stress levels compared to the baseline model, consistent with the higher lateral confinement provided by the high stiffness encasement. Comparing the deviatoric stress-strain curves with the load-displacement responses (Figure 2b) reveals that the onset of column yielding and the mobilization of encasement confinement are not always apparent in the global load-displacement behavior. The load-displacement curves may suggest a continuous increase in the bearing capacity, while the deviatoric stress-strain curves indicate a yielding of the column material and a redistribution of stresses within the GEC system.

These findings highlight the importance of considering the local stress-strain behavior of the column infill when evaluating the performance of GECs. The deviatoric stress-strain relationships provide valuable information on the onset of column failure and the mobilization of encasement confinement, which may not be captured by the global load-displacement response alone.

CONCLUSIONS

This study investigated the performance of geosynthetic encased columns (GECs) in soft soils using physical models with a transparent clay surrogate. The results demonstrated that the tensile strength and stiffness of the encasement play a relevant role in controlling the failure mechanisms and the overall performance of GECs.

In the GEC models tested in very soft soils, the encasement tensile strength proved to be a factor influencing both the failure mechanism and overall system performance. The load-settlement response of the GEC improvement demonstrated greater dependence on the encasement properties than on the shear strength of the column infill material, with the latter remaining constant throughout the study. Notably, higher encasement stiffness led to a more uniform distribution of deformations along the column length and a significant reduction in maximum radial strains.

The mobilized encasement confinement was identified as a key mechanism contributing to the improved performance of GECs compared to unreinforced columns. The encasement confinement enabled a continuous increase in the bearing capacity, provided that the tensile strains remained within the allowable limits. Stiffer encasements led to a more rapid mobilization of confinement at lower axial strains, due to the steeper tensile strength-strain response.

The column infill deviatoric stress-strain relationships were found to provide valuable insights into the local stress-strain behavior of GECs, capturing the onset of column failure and the mobilization of encasement confinement in greater detail than the global load-displacement response. This highlights the importance of considering both local and global performance indicators when evaluating the effectiveness of GEC systems.

REFERENCES

Alexiew, D., Kuster, V., and Assinder, P. (2011). *An Introduction to Ground Improvement using Geotextile Encased Columns (GEC).* 22.

Alexiew, D., and Raithel, M. (2015). Geotextile-Encased Columns, Case Studies over Twenty Years. In *Ground Improvement Case Histories* (pp. 451–477). Elsevier. https://linkinghub.elsevier.com/retrieve/pii/B978008100192900017X.

Ali, K., Shahu, J. T., and Sharma, K. G. (2012). Model tests on geosynthetic-reinforced stone columns: A comparative study. *Geosynthetics International*, 19(4), 292–305.

Ali, K., Shahu, J. T., and Sharma, K. G. (2014). Model tests on single and groups of stone columns with different geosynthetic reinforcement arrangement. *Geosynthetics International*, 21(2), 103–118.

Alkhorshid, N. R., Araujo, G. L. S., Palmeira, E. M., and Zornberg, J. G. (2019). Large-scale load capacity tests on a geosynthetic encased column. *Geotextiles and Geomembranes*, 47(5), 632–641.

Almikati, A., Pierozan, R. C., Sadek, S., and Zornberg, J. G. (2023). Geotechnical Characterization of Laponite as Transparent Clay Surrogate. *Geotechnical Testing Journal*, 46(3), 20220106.

Ayadat, T., and Hanna, A. M. (2005). Encapsulated stone columns as a soil improvement technique for collapsible soil. *Proceedings of the Institution of Civil Engineers - Ground Improvement*, 9(4), 137–147.

Chen, J.-F., Wang, X.-T., Xue, J.-F., Zeng, Y., and Feng, S.-Z. (2018). Uniaxial compression behavior of geotextile encased stone columns. *Geotextiles and Geomembranes*, 46(3), 277–283.

Ghazavi, M., and Nazari Afshar, J. (2013). Bearing capacity of geosynthetic encased stone columns. *Geotextiles and Geomembranes*, 38, 26–36.

Gniel, J., and Bouazza, A. (2009). Improvement of soft soils using geogrid encased stone columns. *Geotextiles and Geomembranes*, 27(3), 167–175.

Hong, Y.-S., Wu, C.-S., and Yu, Y.-S. (2016). Model tests on geotextile-encased granular columns under 1-g and undrained conditions. *Geotextiles and Geomembranes*, 44(1), 13–27.

Malarvizhi, S. N., and Ilamparuthi, K. (2004). Load versus Settlement of Claybed stabilized with Stone & Reinforced Stone Columns. *GeoAsia*.

Miranda, M., and Da Costa, A. (2016). Laboratory analysis of encased stone columns. *Geotextiles and Geomembranes*, 44(3), 269–277.

Miranda, M., Da Costa, A., Castro, J., and Sagaseta, C. (2015). Influence of gravel density in the behaviour of soft soils improved with stone columns. *Canadian Geotechnical Journal*, 52(12), 1968–1980.

Miranda, M., Da Costa, A., Castro, J., and Sagaseta, C. (2017). Influence of geotextile encasement on the behaviour of stone columns: Laboratory study. *Geotextiles and Geomembranes*, 45(1), 14–22.

Murugesan, S., and Rajagopal, K. (2009a). Investigations on the behaviour of geosynthetic encased stone columns. *Stand Alone*, 2411–2414.

Murugesan, S., and Rajagopal, K. (2009b). Shear Load Tests on Stone Columns With and Without Geosynthetic Encasement. *Geotechnical Testing Journal*, 32(1), 101219.

Nazari Afshar, J., and Ghazavi, M. (2014). Experimental Studies on Bearing Capacity of Geosynthetic Reinforced Stone Columns. *Arabian Journal for Science and Engineering*, 39(3), 1559–1571.

Pierozan, R. C., Almikati, A., Araujo, G. L. S., and Zornberg, J. G. (2022). Optical and Physical Properties of Laponite for Use as Clay Surrogate in Geotechnical Models. *Geotechnical Testing Journal*, 45(1), 20210100.

Rajagopal, K., Krishnaswamy, N. R., and Madhavi Latha, G. (1999). Behaviour of sand confined with single and multiple geocells. *Geotextiles and Geomembranes*, 17(3), 171–184.
Wu, C.-S., and Hong, Y.-S. (2009). Laboratory tests on geosynthetic-encapsulated sand columns. *Geotextiles and Geomembranes*, 27(2), 107–120.